Clinical investigation of the Nucleus Slim Modiolar Electrode

Antje Aschendorff[a]   Robert Briggs[f]   Goetz Brademann[b]   Silke Helbig[c]
Joachim Hornung[d]   Thomas Lenarz[e]   Mathieu Marx[g]   Angel Ramos[j]
Timo Stöver[c]   Bernard Escudé[h]   Chris J. James[g, i]

[a]University of Freiburg, Freiburg, [b]Universitätsklinikum Schleswig-Holstein, Kiel, [c]Klinikum der J.W. Goethe-Universität, Frankfurt, [d]Universitätsklinikum Erlangen, Erlangen, and [e]Medizinische Hochschule Hannover, Hannover, Germany; [f]University of Melbourne, Melbourne, VIC, Australia; [g]Centre Hospitalier Universitaire de Toulouse, [h]Clinique Pasteur Toulouse, and [i]Cochlear France SAS, Toulouse, France; [j]Complejo Hospitalario Universitario Insular Materno Infantil, Las Palmas, Spain

Abstract
Aims: The Nucleus CI532 cochlear implant incorporates a new precurved electrode array, i.e., the Slim Modiolar electrode (SME), which is designed to bring electrode contacts close to the medial wall of the cochlea while avoiding trauma due to scalar dislocation or contact with the lateral wall during insertion. The primary aim of this prospective study was to determine the final position of the electrode array in clinical cases as evaluated using flat-panel volume computed tomography. ***Methods:*** Forty-five adult candidates for unilateral cochlear implantation were recruited from 8 centers. Eleven surgeons attended a temporal bone workshop and received further training with a transparent plastic cochlear model just prior to the first surgery. Feedback on the surgical approach and use of the SME was collected via a questionnaire for each case. Computed tomography of the temporal bone was performed postoperatively using flat-panel digital volume tomography or cone beam systems. The primary measure was the final scalar position of the SME (completely in scala tympani or not). Secondly, medial-lateral position and insertion depth were evaluated. ***Results:*** Forty-four subjects received a CI532. The SME was located completely in scala tympani for all subjects. Pure round window (44% of the cases), extended round window (22%), and inferior and/or anterior cochleostomy (34%) approaches were successful across surgeons and cases. The SME was generally positioned close to the modiolus. Overinsertion of the array past the first marker tended to push the basal contacts towards the lateral wall and served only to increase the insertion depth of the first electrode contact without increasing the insertion depth of the most apical electrode. Complications were limited to tip fold-overs encountered in 2 subjects; both were attributed to surgical error, with both reimplanted successfully. ***Conclusions:*** The new Nucleus CI532 cochlear implant with SME achieved the design goal of producing little or no trauma as indicated by consistent scala tympani placement. Surgeons should be carefully trained to use the new deployment method such that tip fold-overs and over insertion may be avoided.

© 2017 S. Karger AG, Basel

Chris J. James
Cochlear France SAS
135 Route de Saint Simon
FR–31100 Toulouse (France)
E-Mail cjames@cochlear.com

Introduction

Cochlear implants (CI) have become the most successful of all implantable sensory prostheses and the standard of care for the majority of individuals with severe to profound hearing loss. Children with profound congenital hearing loss have been able to develop excellent speech and language and the majority attend mainstream schools [Venail et al., 2010]. The majority of established CI users are now able to use the telephone [Tan et al., 2012]. Refinements to hardware and surgical technique have continued over the years in many ways, both contributing to improved outcomes.

The active electrode array is a key component of any CI system as it provides the interface between the prosthesis and the auditory system of the recipient. Modern multichannel CI use an array of electrodes inserted into the scala tympani (ST) of the cochlea in order to provide spectral information through selective stimulation of electrodes positioned close to the target spiral ganglion cells (SGC), exploiting the natural tonotopic organization of the cochlea, with low-frequency information being delivered to the most apical electrodes and higher frequencies more basally. However, although the implanted electrode arrays may have more than 20 electrode contacts, it is well known that the stimulation fields of individual electrode contacts are quite broad, so that neural populations stimulated by adjacent monopolar electrodes overlap considerably [Hughes and Abbas, 2006]. This "spread of excitation" (or "channel interaction") reduces the spectral resolution and limits the potential advantage of having a large number of electrodes.

Many multichannel CI, such as the Nucleus CI522, use electrodes that are straight prior to insertion. Such arrays tend to take up position mostly along the outer (lateral) wall of the ST (Fig. 1a), and the electrode contacts are therefore some distance from the modiolus and the spiral ganglion. Several precurved arrays, such as the Nucleus Contour Advance, which in an ideally adopt a position close to the modiolar wall, have been introduced (Fig. 1b). The principal rationale of developing such "perimodiolar" electrode arrays is that the contacts are situated closer to the target SGC so that the required stimulation levels are lower than with straight arrays. More importantly, however, the spread of excitation is anticipated to be less with perimodiolar arrays than with straight arrays, due to closer proximity to the SGC. This may provide superior place-pitch spectral discrimination and therefore optimal speech recognition performance.

Several studies have demonstrated lower stimulation thresholds for permodiolar arrays than for straight arrays, either when measured psychophysically or when assessed by objective measures [Cohen et al., 2001; Gordin et al., 2009; Runge-Samuelson et al., 2009; Jeong et al., 2015; Müller et al., 2015; Telmesani and Said, 2015]. Other studies have reported a reduced spread of excitation using forward masking ECAP paradigms [Hughes and Abbas, 2006; Basta et al., 2010; Hughes and Stille, 2010] with improved spectral discrimination. Taken together, these studies demonstrate that perimodiolar electrode arrays achieve their primary design goals.

The closeness of the array to the modiolus, or medial-lateral position, has been characterized using a number of methods. Holden et al. [2013] described a wrapping factor (WF) as the ratio of the active length of the electrode array (from the most basal to the most apical electrode contact) and the length along the lateral wall of the ST over the corresponding angle as measured from computed tomography imaging (Fig. 1d). A straight (lateral wall) array will have a WF close to 1, whereas a perimodiolar array will take a shorter path and the WF can be as low as 0.5. As an example, the WF is 0.89 for the CI522 in Figure 1a and 0.60 for the CI532 in Figure 1c. In a group of 59 subjects with confirmed ST electrode array placements, Holden et al. [2013] found a statistically significant correlation between WF and monosyllable recognition score (asymptote of performance over 2 years post-activation); higher scores were associated with lower WF.

The medial-lateral position can also be characterized by the angle travelled per millimeter of active length of the array (AT). In the examples given in Figure 1a–c, the AT for the CI522 is 18°/mm, compared to 30°/mm for the CI532. Direct measures of electrode-to-modiolus distance, even from the best-quality CT imaging available, are problematic due to residual electrode artefacts blurring the boundary of the medial wall. Some studies, such as that of Esquia Medina et al. [2013], have used the distance between the electrode contact and the center of the modiolus (EMD) as a surrogate measure. Esquia Medina et al. [2013] found a statistically significant correlation between monosyllabic word scores and EMD; higher scores were associated with contacts being closer to the modiolus; however, Van der Beek el al. [2016] found only a trend using EMD defined by the distance from the electrode contact to the nearest point on the medial wall as identified in images. The range of AT would have been approximately 10–24°/mm in their study, with higher AT values indicating smaller EMD. AT and EMD may better characterize the medial-lateral placement of an electrode

Fig. 1. Cone beam images of electrode arrays in situ, in vivo. Images are shown for 3 types of nucleus electrode arrays in the ideal position: Slim Straight (CI522) (**a**), Contour Advance (CI512) (**b**), and Slim Modiolar (CI532) (**c**). **d** Schema for analysis of the medial-lateral position of the array: the insertion depth (angle) of electrode contacts E1 and E22, distance A (the horizontal dotted line), and the corresponding spiral arc length along the lateral wall (curved dashed line). **a–c** Images are courtesy of Tobias Struffert, University of Erlangen, Germany.
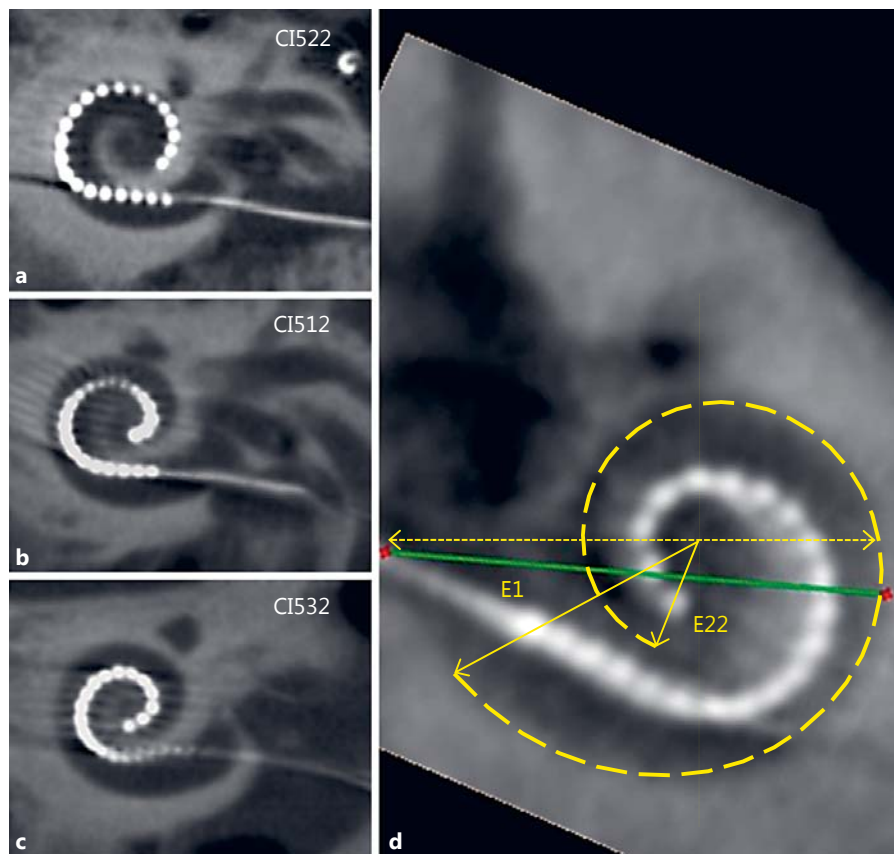
array since they do not include cochlear size in their derivation.

Holden et al. [2013] also reported cases in which the electrode array had been inserted directly into the scala vestibuli (SV) or translocated from the ST into the SV. Such translocation has been reported in several other studies and may be more common with perimodiolar arrays than with straight arrays [Wanna et al., 2014]. Translocation is also associated with poorer outcomes compared to when the array remains within the ST [Aschendorff et al., 2007; Finley et al., 2008]. Successful ST insertion appears to depend on the surgical technique to a significant degree [Aschendorff et al., 2007], but it seems reasonable to assume that device design is another important factor.

The aim of the present study was to evaluate the insertion characteristics and associated outcomes of a new perimodiolar electrode array. The Nucleus CI532 uses the same receiver-stimulator as the other current CI500 series devices (CI512 and CI522) coupled to the new Slim Modiolar electrode (SME) array. The new array was based on previous multicenter studies of a prototype design in-

vestigating feasibility [Briggs et al., 2011]. Unlike the Nucleus Contour Advance electrode, the precurved shape of the SME is kept straight by a thin external sheath prior to insertion rather than using an internal stylet. The SME uses the half banded electrodes as for the Contour Advance, but it has a diameter of 0.5 mm at the position of the most basal electrode, reducing to 0.4 mm at the apex (the corresponding dimensions of the Contour Advance are 0.8 and 0.5 mm). This gives the SME a cross sectional area about 40% that of the Contour Advance.

Figure 2 shows the SME and the external sheath at various stages of insertion. The electrode array is first drawn back (Fig. 2a) into the sheath (orange) and then the array and the sheath are inserted (via cochleostomy or round window [RW]) to about 5 mm. The array is then further advanced through the sheath until it is fully inserted (Fig. 2b) and then the sheath is retracted and discarded (Fig. 2c). In Figure 2c, 3 "markers" are visible proximal to the stimulating contacts. These are used to indicate the insertion depth.

High-quality in vivo imaging of the temporal bone with an electrode array in place is challenging due to me-
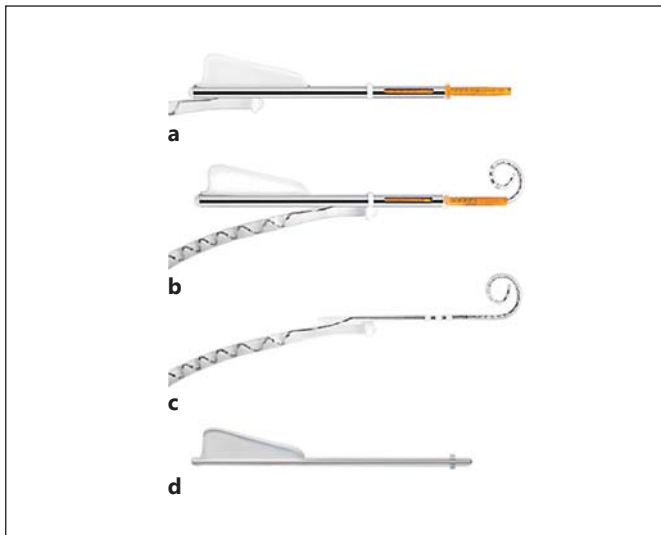
Fig. 2. Slim Modiolar electrode with the array loaded in the sheath (**a**) and then advanced through the sheath (**b**) and with the sheath removed as in the final situation (**c**). A cochleostomy sizing tool (**d**) is provided with the implant.

tallic (blooming) artefacts [Yang et al., 2000], and confirmation of the scalar position is particularly difficult due to the need to resolve soft tissue details. The scalar position of straight and perimodiolar electrode arrays was identified using multiplanar reconstruction of high-resolution 64-slice multidetector CT [Lane et al., 2007], but the results were equivocal in many cases. Alternatively, several studies have coregistered pre- and postoperative high-resolution images, thereby showing electrode contact positions together with fine structural details [Skinner, 2007; Schuman et al., 2010; Holden et al., 2013]. Unfortunately, however, both of these methods are time consuming and require relatively high radiation doses.

In the present study, we used flat-panel volume (FPV) CT scanning to identify the scalar position of the SME postoperatively. This technique is essentially equivalent to so-called "cone beam CT" (CBCT), "digital volume tomography," and "rotational tomography," all of which use similar reconstruction algorithms. These techniques are superior to conventional helical high-resolution computed tomography as the metallic artefacts produced by the electrode contacts are largely eliminated and ST and SV are visible up to at least one and half turns of the cochlea [Marx et al., 2014]. Successful identification of the CI electrode scalar position has also been reported in temporal bone studies [Husstedt et al., 2002; Ruivo et al., 2009; Cushing et al., 2012; Saeed et al., 2014] and in vivo

postoperative studies [Aschendorff et al., 2007]. Another important advantage of FPV CT for in vivo applications is that it offers reduced exposure to ionizing radiation compared to conventional helical high-resolution computed tomography [Faccioli et al., 2009; Ruivo et al., 2009].

Several studies have reported rates of electrode array translocation (from ST to SV) with the Contour Advance, as measured using high-resolution FPV CT [Aschendorff et al., 2007; Coordes et al., 2013; Wanna et al., 2014]. The lowest reported incidence of translocation was 19%. The aim of our study was to estimate the translocation rate of the SME. Additional measurements were also made from the imaging, such as insertion depth angles for the first and last electrode contacts and the medial-lateral position, as well as cochlear size (distance A [Escudé et al., 2006]).

Methodology

Study Design
This was a prospective, single arm, multicenter observational study of 45 adults implanted with a Nucleus CI532 device. There were 8 study centers in total from Germany (Freiburg, Kiel, Erlangen, Hannover, and Frankfurt), France (Toulouse), Spain (Las Palmas), and Australia (Melbourne, VIC). The centers were selected on the basis of extensive CI experience, access to a sufficient number of potential CI532 recipients, and the presence of appropriate imaging facilities. In our study we hypothesized a translocation rate of less than 20% with the SME. A power calculation was therefore performed on this basis, which suggested a minimum subject number of 45, allowing for a 10% attrition rate.

The principal aims of the study were to characterize the final position of the SME and record surgical experiences with the device. This study also recorded longer-term outcomes with the CI532, including speech recognition, subjective benefits, and hearing preservation. However, these measures are outside of the scope of this paper and will be submitted in a follow-up report.

Study Participants
Participants were 18 years of age or older at the time of implantation, conventional candidates for unilateral CI according to local criteria, and native speakers in the local language. In addition to the normal contraindications for cochlear implantation (e.g., psychosocial considerations, existing medical conditions, and anatomical irregularities), the following exclusion criteria were applied: evidence of hearing loss prior to 5 years of age; prior cochlear implantation in either ear; ossification or any other cochlear anatomical abnormality, such as common cavity, that might prevent complete and normal insertion of the electrode array; hearing impairment due to a lesion or neuropathy of the VIII nerve or central auditory pathways; unrealistic expectations regarding the possible benefits, risks, and limitations inherent to the surgical procedure(s) and prosthetic device; and unwillingness or inability to comply with all investigational requirements such as undergoing a postoperative CBCT scan.

Approval for this study was obtained from the local ethics committees and competent authorities for all 8 centers. Patients gave their informed consent to participate in this study.

Surgeon Device Familiarization

Prior to this study, the investigational surgeons attended a training workshop during which they were introduced to the device and recommended surgical technique, including an overview of anticipated use errors and potential complications related to electrode array insertion. Each investigator also performed practice insertions into real temporal bones and a plastic model, using both RW and cochleostomy approaches. These insertions were video recorded so that the surgeons could compare their technique with that described in the Physician's Guide for the CI532. Further training was provided immediately prior to the first surgeries such that the surgeon was required to successfully insert the electrode array 5 times into a plastic model.

Surgical Questionnaire

Outside of the recommendations covered the CI532 Physician's Guide, surgeons were free to conduct other aspects of the surgery according to their preferences and local practice. This included details such as facial recess size, the position of the cochlear opening, and use of lubrication, antibiotics, and steroids. This information was recorded in a detailed surgical questionnaire for each case shortly after each surgery. Many details were intended to provide reference information in case of unexpected intra- or postoperative complications, but certain key questions relating to insertion of the electrode array were intended for evaluation in this study. There were additional questions about the ease of handling of the sheath, electrode array insertion, and electrode array insertion depth relative to markers.

Intra- and Postoperative Imaging and Analysis

Plain X-ray or fluoroscopy was performed after each electrode insertion in order to confirm satisfactory positioning and, in particular, to indicate any presence of electrode tip fold-over which would suggest the need for reinsertion or use of a back-up device.

CBCT scans were taken within 1 month of surgery. A variety of different cone beam scanners was available at the different study centers, but the following imaging parameters were recommended: 80–125 kV and 7–50 mA, with a 360° rotation of 18–40 s (pulsed). Projection images were obtained from a cylindrical volume of 7–8 cm (height) by 7–8 (single temporal bone) or 12–15 cm (diameter) (both temporal bones), with a calculated effective dose of <150 μSv. Image data were used to generate a 3-D volumetric (DICOM) dataset with an isometric voxel size <300 μm.

Reconstructed images were examined at each study center for scalar position of the individual electrode contacts and measurement of the overall insertion angle [Xu et al., 2000; Verbist et al., 2010] for most apical and most basal contacts. The measurements made at each study center were subsequently verified (blindly) by the coordinating investigator (A.A.) and consultant radiologist (B.E.). Thus the scala position was verified by 2 independent observers.

CBCT images were further examined in order to document the closeness of modiolar approximation by the electrode array in situ. This measurement was based on the method described by Holden et al. [2013], in which the mediolateral position is quantified by a WF, i.e., the ratio of the length of the active electrode array and the lateral wall length over the same angular distance. Medial-lateral position in the present study was characterized by a similar but simplified method which we denoted MP: two dimensional reconstructions were prepared of each implanted cochlea on a near-coronal plane as described by Escudé et al. [2006]. This projection captured the entire basal turn so that the largest diameter, i.e., distance A, could be measured (Fig. 1d, horizontal dotted line). A spiral template derived from Escudé et al. [2006] (equation 1) was used to locate the center of the cochlear spiral such that the angles of the most basal electrode contact E1 and the most apical electrode contact E22 could be determined. Using equation 3 from Escudé et al. [2006], the length of the lateral wall from 0° to E1 and then from 0° to E22 could be calculated. In derivation of the MP here, the active length of the curved array was 13.4 mm from engineering specifications (Cochlear Ltd., Macquarie University, Australia). Thus, MP was defined as 13.4 mm divided by the difference in corresponding lateral wall length from E22 to E1 in millimeters (Fig. 1d, curved dashed line). Similarly, AT was the difference in angle E1 to E22 divided by 13.4 mm.

The electrode positioning of 10 Melbourne subjects were also measured using the WF method described by Holden et al. [2013] in order to assess agreement with the simplified MP measure described above. We note that the method of Holden et al. [2013] requires preoperative CT scans in addition to postoperative CT scans and specific software and technical skills.

In addition to the quantitative assessment of modiolar proximity, a subjective assessment of the coronal images was made by categorizing the quality of perimodiolar placement as follows: good = perimodiolar position with little or no dark space on the medial side of the array; moderate = a definite area of dark space on the medial side of the array, but with all electrode contacts closer to the medial wall; poor = an array with any electrodes closer to the lateral wall than the medial wall (this typically occurred between 45° and 180°). Examples of each category are shown in Figure 3.

Results

Investigational Subjects

Forty-five patients (22 males and 23 females) were recruited for this study and implanted with the CI532. The mean age at implantation was 60.7 years (SD 14.6, range 24–89). The etiology was unknown in 33 cases, and it was Meniere's disease, familial hearing loss, otosclerosis, chronic otitis media, or noise-induced hearing loss for the remaining subjects. Hearing loss was progressive in 38 cases, sudden in 5 cases, and congenital in 2 cases.

Surgical Questionnaire

Questionnaires were returned for all initial surgeries, though not all questions were answered in every case. Twenty-three left ears and 22 right ears were implanted. The facial recess was extended in 9 (20%) cases, and the posterior canal wall was thinned in 25 (56%) cases. The

Table 1. Responses to surgical questionnaire items relating to sheath handling and electrode insertion

	AS	A	N	D	DS
Loading of the electrode into the sheath was uncomplicated	31	12	0	1	1
Insertion of the sheath into the cochlea was uncomplicated	18	16	6	3	2
Advancing the electrode through the sheath was uncomplicated	26	17	1	1	0
The stopper was stable during insertion	30	12	2	1	0
The stopper prevented overinsertion of the sheath	22	17	4	2	0
Removal of the sheath was uncomplicated	24	14	3	4	0

Total: n = 45 in each case. AS, agree strongly; A, agree; N, neutral; D, disagree; DS, disagree strongly.
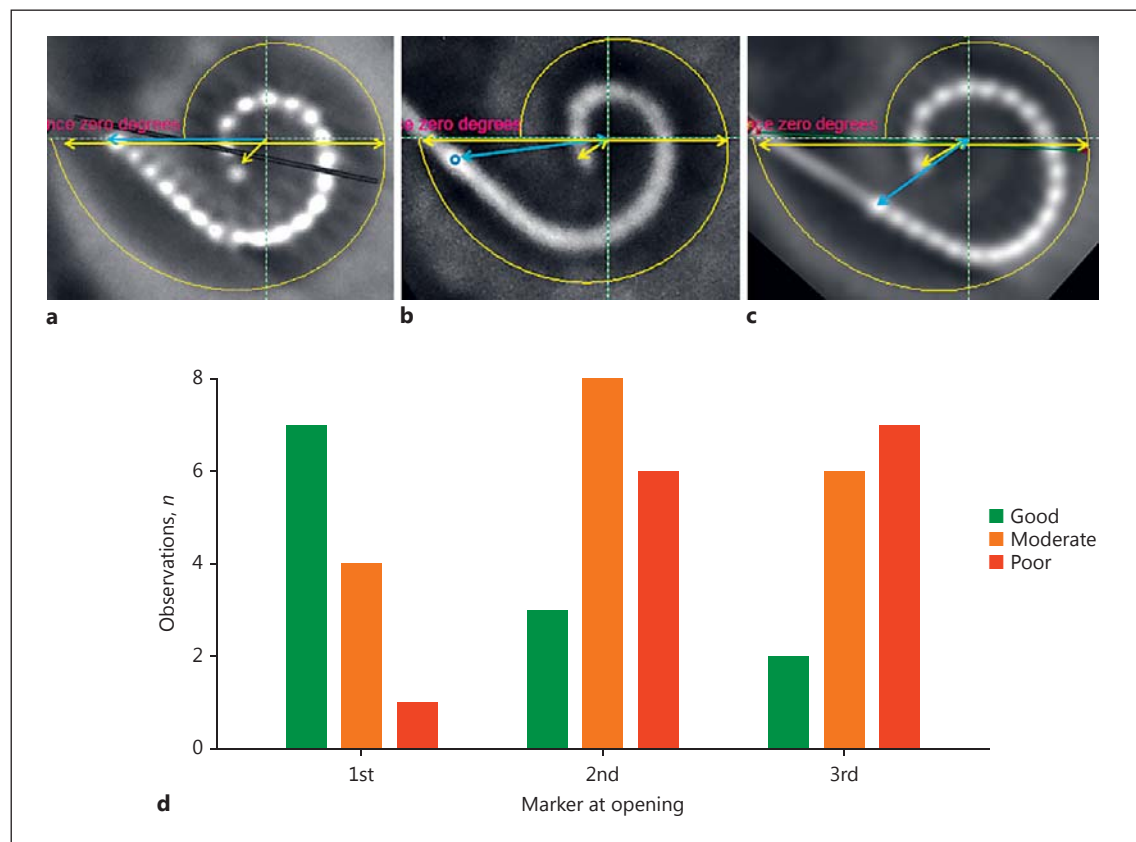
Fig. 3. Coronal section cone beam CT images showing left to right examples of good (**a**), moderate (**b**), and poor (**c**) electrode medial-lateral positions. **d** Relationship between marker position and subjective medial-lateral position.

mean estimated dimensions of the facial recess opening were 2.9 mm (SD 1.1) by 5.7 mm (SD 1.6).

Insertion was via a RW incision in 44% of the cases, with a further 22% via an extended RW and 16, 13, and 4% via inferior, anterior-inferior, and anterior cochleostomy, respectively. The proportions of cochlea openings of <0.8, 0.8–1.0, and >1.0 mm were 9, 84, and 7%, respec-

tively, and the sizing tool (Fig. 2d) was used to gauge the appropriate cochleostomy opening size in 84% of the cases. Healon™ lubricant was used in 16 (36%) insertions.

Responses to a number of key questions related to the ease of sheath handling and electrode insertion are shown in Table 1. These responses suggested a majority of satisfactory experiences with loading of the electrode into the

Aschendorff et al.

Table 2. Summary statistics of cochlear diameter and electrode contact positions (n = 44)

	Mean (SD)	Minimum	Maximum	Median
Medial-lateral position	0.62 (0.05)	0.54	0.77	0.61
Distance A, mm	8.9 (0.4)	7.9	9.6	9.0
E1 angle, degrees	18 (14)	0	55	15
E22 angle, degrees	403 (32)	295	455	405
Active angle, degrees	388 (32)	265	430	395
Angle per millimeter, degrees	28.9 (2.3)	20.0	32.0	29.0

sheath, insertion of the sheath into the cochlea, and removal of the sheath after advancement of the electrode. Insertion and removal of the sheath did not appear to be systematically more difficult in round window insertions. The sheath and electrode array was inserted and then removed and reinserted in 3 cases due to resistance to insertion of the sheath. In 2 of these cases the RW overhang appeared to be the source of resistance and was removed before reinsertion. This indicates that some care and experience are necessary with the new array such that there is adequate opening of the cochlea. Once inserted, the electrode array was further manipulated after removal of the sheath in 9 cases, with the electrode being pushed in further in 6 cases (see Interoperative Imaging). These manipulations were not specifically related to improvement of the implanted electrode position – they were more about handling the lead wire position.

Intraoperative Imaging

Intraoperative plain X-ray imaging indicated a satisfactory initial electrode position in 40 out of 45 cases. In 1 case, the array was initially inserted to the first marker but then inserted more deeply following the viewing of the X-ray. In another case, since X-ray was not available the surgeon chose to withdraw the electrode array, reload, and reinsert due to considerable resistance during the first removal of the sheath. A satisfactory position was confirmed by digital volume tomography the following day. In 1 further case the array came out of the cochlea during fixation of the lead wires. The array was reloaded and reinserted.

In 2 cases an electrode tip fold-over was apparent from intraoperative X-ray. In one of these, the array was withdrawn, reloaded, and reinserted, resulting in an apparently satisfactory insertion. However, high-resolution CBCT imaging the following day again showed a tip fold-over, and the patient was reimplanted successfully with a CI512 device (Contour Advance electrode). Accordingly, this subject was excluded from further study analysis. In the other case, CBCT imaging confirmed the tip fold-over

and the subject was subsequently reimplanted successfully with a second CI532. It is understood that intraoperative imaging is not a standard procedure in all centers; however, considering the uniqueness of this device and insertion technique its use is advisable during the initial surgeries as an aid to understanding and refining a newly learned technique.

The likely cause of tip fold-overs was determined from a review of video recordings and in discussion with the surgeons. One tip fold-over was caused by incorrect orientation of the electrode array with respect to the plane of the basal turn during insertion and the other by over-insertion of the electrode sheath due to the stopper going into a particularly large round window opening.

Postoperative CBCT Imaging

Digital primary reconstruction data files were obtained for all 44 patients who finally received a Nucleus CI532 CI. The data were subject to at least 2 independent reviews – by the implanting center, by the coordinating investigator, or by the consultant radiologist. The opinion was unanimous in 42 out of 44 cases. In the 2 remaining cases the consultant radiologist indicated that the scalar position of the electrode array could not be definitively determined due to poor image quality. However, in these 2 cases the scalar locations determined by the center and the coordinating investigator were in agreement.

From these examinations, the electrode array was determined as being located completely in ST in all 44 cases, with no cases of primary SV insertions or translocation out of ST.

Analysis of Array Position

Summary statistics of the measures for calculation of MP in all 44 data sets are provided in Table 2. The mean insertion angle from the center of the RW to the most apical electrode was 402.7° (SD 31.8°, range 295–455°). MP values ranged from 0.54 to 0.77, with a mean of 0.62. The AT was generally >20°/mm, with a median of 29°/mm (Table 2); however there was an outlier case with an inser-
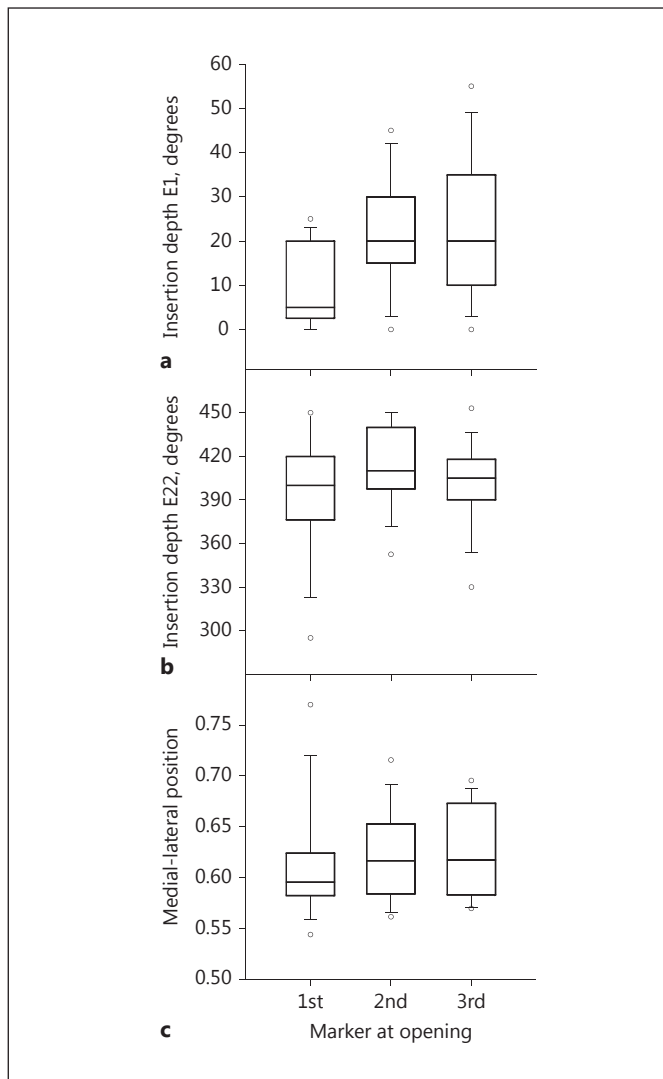
Fig. 4. Relationship between marker position and the insertion depth of E1 (**a**), the insertion depth of E22 (**b**), and the medial-lateral position (**c**). Medians, 25–75th percentiles, 10–90th percentiles, outliers.

tion depth of 295° where the AT was 20°/mm. We can only speculate that in this case the array was hung up on some feature or obstruction in ST.

In addition to the calculations of MP, the CBCT reconstructions of 9 of the subjects implanted in Melbourne were also used to calculate the WF using the methodology of Holden et al. [2013]. WF and MP values were found to be highly correlated ($R^2 = 0.684$). However, there was an average bias, with MP being on average 0.035 greater than the WF of Holden et al. [2013]. Thus it could be concluded that MP values appear to provide a slightly

conservative estimate of the medial-lateral position. The differences would lie in the estimation of the lateral wall length which in the case of the WF was derived from coregistration of an anatomical model with the CT image of the contralateral ear; the fitted template spiral used in the MP may have slightly underestimated the length due to the limited bone/scala contrast.

The relationships between the final position of the depth markers on the electrode array and the achieved insertion depths for basal and apical electrodes and medial-lateral position (MP) measures were also examined, and these are shown in Figure 4. Arrays were inserted to the first, second, and third markers in 12, 17, and 15 cases, respectively.

Fuller insertion, as indicated by the markers, was associated with a significant increase (Kruskal-Wallis ANOVA on ranks, $p < 0.05$) in the insertion depth of the most basal electrode (E1), as might be anticipated (Fig. 4a). However, insertion to the second or third marker did not result in a greater insertion depth of the most apical electrode (E22) relative to that obtained from insertion to the first marker (Fig. 4b). The median MP was lowest (best) for insertions to the first marker but MP was somewhat insensitive to marker position (Fig. 4c).

Subjective Assessment of Perimodiolar Placement

The array position was deemed good, moderate, and poor in 12, 18, and 14 cases, respectively. Figure 3a–c shows examples of arrays from each category.

The relationship between insertion marker position and subjective assessment of the perimodiolar position is shown in Figure 3. It is evident that insertion to the second and third markers resulted in a systematic decrease in the proportion of good electrode positions and an increase in the proportion of poor positions.

Discussion

The primary endpoint measure of scalar location from FPV CT demonstrated complete ST localization in all cases. This suggests that cochlear implantation with the SME array results in a low level of intracochlear trauma. Thus, one primary design goal of the SME was achieved. However, there were 2 cases in which the initial insertion of the array resulted in a tip fold-over.

The thinness and flexibility of the array may make it more prone to tip fold-over and to reduction of any force that can be applied to the array which could induce trauma. Analysis of surgical videos identified that the mech-

Aschendorff et al.

anism for the tip fold-overs was related to use errors as outlined in the Physician's Guide for the device. In one case the surgeon actively deviated from the surgical guidance for their first CI532 case, orienting the electrode such that it deployed posterior to the plane of the cochlea, which resulted in a fold-over identified postoperatively. That subject was subsequently reimplanted with a CI512 device. All subsequent CI532 surgeries by this surgeon were performed successfully and without incident. The second case was a large RW opening resulting in the stopper entering the cochlea, which was not noticed by the surgeon. That subject was successfully reimplanted with a CI532 device, with the surgeon in this case keeping the stopper level with the RW opening as per the Physician's Guide. Reports of fold-over in literature vary between 0.8–5.6% for all electrode types/manufacturers as follows: 0.8% [Dirr et al., 2013], 2% [Zuniga et al., 2017], and 5.6% [Grolman et al., 2009]. The large range in reporting is likely attributed to the design of the studies, which in many cases were retrospective case reviews [Dirr et al., 2013; Zuniga et al., 2017] and therefore only captured fold-overs left in situ, as opposed to prospective studies [Grolman et al., 2009] reporting fold-overs identified intraoperatively. The rate of 4.4% (2 out of 45) identified in the current study is representative of a prospective approach rather than the retrospective case reviews which typically report lower rates of fold. Confirmed use errors such as those seen here can be addressed via training and we expect that with experience fold-over rates will decrease over time.

In other surgeries it was noted that the sheath needed to be carefully held steady to avoid the sheath stopper entering the opening during advancement of the array through the sheath. Conversely in a number of cases overall access was more difficult. The bony overhang needed to be more fully removed to allow smooth introduction of the sheath, and in some cases the sheath assembly made full visualization of the cochlea opening difficult.

The SME performed well on several measures of medial-lateral placement, with mean MP of 0.62. The average angle travelled per millimeter of active array (AT) was 29°/mm which would indicate low electrode contact to modiolus distances. The mean MP was at the lower end of the range reported by Holden et al. [2013], and the AT was generally greater than those obtained for straight arrays [Esquia Medina et al., 2013].

It appeared that advancing the array past the first marker position into the cochlea opening is undesirable since it does not result in greater total insertion depths and only serves to increase the insertion depth of the first electrode contact E1 and move basal electrodes away from the modiolus. Holden et al. [2013] also found that the insertion depth angle for the most basal electrode was negatively correlated with performance (range 2–231°) [Holden, pers. commun.]. This may have been due to incomplete use of the basal part of the modiolus or to an increased electrode-to-modiolus distance for basal electrodes as seen in the examples given here (Fig. 3c). Van der Beek et al. [2005] noted that deep insertion of the Clarion HiFocus 1 without a positioner tended to increase the electrode-to-modiolar distance for basal contacts and it increased the insertion depth angles. They speculated that, although the total insertion depth in these cases was similar to that achieved with the positioner, the increased insertion depth for the most basal electrode contacts may have led to poorer speech recognition compared to that obtained with the positioner.

The "bulging" effect of overinsertion of perimodiolar electrodes was previously noted by James et al. [2005] for the Contour Advance, and Escudé et al. [2006] confirmed that this effect could be measured in smaller cochleae. The average cochlea size measured by distance A was 9.23 mm in the study of Escudé et al. [2006] and 8.85 mm in a study by Van der Marel et al. [2014], and these values were similar to the average of 8.90 mm found in the current study. The results of the present study suggest that in order to obtain consistent perimodiolar placement in the basal and in the apical regions the array does not need to be advanced past the first marker. Temporal bone work suggests that the array will take up its natural position for larger cochleae by pulling itself in using the natural tension in the curve of the array.

The CI532 has the first commercial sheath-based deployment system for a perimodiolar electrode. The sheath design allows for significant reduction of the electrode diameter and facilitates a more controlled insertion technique such that the electrode can only advance through the sheath without contact with the lateral wall, reducing the potential for trauma. This unique design and insertion technique does, however, require training and experience developed over time using the device clinically. Even within this study we saw learning effects resulting in adjustment and improvement of the surgical approach over time to adapt to the unique design/technique.

Conclusions

The new electrode array incorporated into the Nucleus CI532 CI achieved the design goal of producing no trauma, as indicated by 100% ST placement, whilst also achieving consistent and close modiolar proximity. As with any new medical device, surgeons should be carefully trained to use the new deployment method to avoid complications and achieve optimal placement.

Acknowledgments

Disclosure Statement

C.J.J. is an employee of Cochlear, the manufacturer of the Nucleus CI532. The other authors report no conflict of interests.

References

Aschendorff A, Kromeier J, Klenzner T, Laszig R: Quality control after insertion of the nucleus contour and contour advance electrode in adults. Ear Hear 2007;28:75S–79S.

Basta D, Todt I, Ernst A: Audiological outcome of the pull-back technique in cochlear implantees. Laryngoscope 2010;120:1391–1396.

Briggs RJS, Tykocinski M, Lazsig R, Aschendorff A, Lenarz T, Stöver T, et al: Development and evaluation of the modiolar research array – multi-centre collaborative study in human temporal bones. Cochlear Implants Int 2011; 12:129–139.

Cohen LT, Saunders E, Clark GM: Psychophysics of a prototype peri-modiolar cochlear implant electrode array. Hear Res 2001;155:63–81.

Coordes A, Ernst A, Brademann G, Todt I: Round window membrane insertion with perimodiolar cochlear implant electrodes. Otol Neurotol 2013;34:1027–1032.

Cushing SL, Daly MJ, Treaba CG, Chan H, Irish JC, Blaser S, et al: High-resolution cone-beam computed tomography: a potential tool to improve atraumatic electrode design and position. Acta Otolaryngol 2012;132:361–368.

Dirr F, Hempel JM, Krause E, Müller J, Berghaus A, Ertl-Wagner B, et al: Value of routine plain X-ray position checks after cochlear implantation. Otol Neurotol 2013;34:1666–1669.

Escudé B, James CJ, Deguine O, Cochard N, Eter E, Fraysse B: The size of the cochlea and predictions of insertion depth angles for cochlear implant electrodes. Audiol Neurotol 2006; 11(suppl 1):27–33.

Esquia Medina GN, Borel S, Nguyen Y, Ambert-Dahan E, Ferrary E, Sterkers O, et al: Is electrode-modiolus distance a prognostic factor for hearing performances after cochlear implant surgery? Audiol Neurotol 2013;18: 406–413.

Faccioli N, Barillari M, Guariglia S, Zivelonghi E, Rizzotti A, Cerini R, et al: Radiation dose saving through the use of cone-beam CT in hearing-impaired patients. Radiol Med 2009;114: 1308–1318.

Finley CC, Holden T, Holden LK, Whiting BR, Chole R, Neely GJ, et al: Role of electrode placement as a contributor to variability in cochlear implant outcomes. Otol Neurotol 2008;29:920–928.

Gordin A, Papsin B, James A, Gordon K: Evolution of cochlear implant arrays result in changes in behavioral and physiological responses in children. Otol Neurotol 2009;30: 908–915.

Grolman W, Maat A, Verdam F, Simis Y, Carelsen B, Freling N, Tange RA: Spread of excitation measurements for the detection of electrode array foldovers. Otol Neurotol 2009;30:27–33.

Holden LK, Finley CC, Firszt JB, Holden TA, Brenner C, Potts LG, et al: Factors affecting open-set word recognition in adults with cochlear implants. Ear Hear 2013;34:342–360.

Hughes ML, Abbas PJ: Electrophysiologic channel interaction, electrode pitch ranking, and behavioral threshold in straight versus perimodiolar cochlear implant electrode arrays. J Acoust Soc Am 2006;119:1538–1547.

Hughes ML, Stille LJ: Effect of stimulus and recording parameters on spatial spread of excitation and masking patterns obtained with the electrically evoked compound action potential in cochlear implants. Ear Hear 2010; 31:679–692.

Husstedt HW, Aschendorff A, Richter B, Laszig R, Schumacher M: Nondestructive three-dimensional analysis of electrode to modiolus proximity. Otol Neurotol 2002;23:49–52.

James CJ, Albegger K, Battmer R, Burdo S, Deggouj N, Deguine O, et al: Preservation of residual hearing with cochlear implantation: how and why. Acta Otolaryngol 2005;125: 481–491.

Jeong J, Kim M, Heo JH, Bang M-Y, Bae MR, Kim J, et al: Intraindividual comparison of psychophysical parameters between perimodiolar and lateral-type electrode arrays in patients with bilateral cochlear implants. Otol Neurotol 2015;36:228–234.

Lane JI, Witte RJ, Driscoll CLW, Shallop JK, Beatty CW, Primak AN: Scalar localization of the electrode array after cochlear implantation: clinical experience using 64-slice multidetector computed tomography. Otol Neurotol 2007;28:658–662.

Marx M, Risi F, Escudé B, Durmo I, James CJ, Lauwers F, et al: Reliability of cone beam computed tomography in scalar localization of the electrode array: a radio histological study. Eur Arch Otorhinolaryngol 2014;271:673–679.

Müller A, Hocke T, Mir-Salim P: Intraoperative findings on ECAP-measurement: normal or special case? Int J Audiol 2015;54:257–264.

Ruivo J, Mermuys K, Bacher K, Kuhweide R, Offeciers E, Casselman JW: Cone beam computed tomography, a low-dose imaging technique in the postoperative assessment of cochlear implantation. Otol Neurotol 2009;30: 299–303.

Runge-Samuelson C, Firszt JB, Gaggl W, Wackym PA: Electrically evoked auditory brainstem responses in adults and children: effects of lateral to medial placement of the nucleus 24 contour electrode array. Otol Neurotol 2009;30:464–470.

Saeed SR, Selvadurai D, Beale T, Biggs N, Murray B, Gibson P, et al: The use of cone-beam computed tomography to determine cochlear implant electrode position in human temporal bones. Otol Neurotol 2014;35:1338–1344.

Schuman TA, Noble JH, Wright CG, Wanna GB, Dawant B, Labadie RF: Anatomic verification of a novel method for precise intrascalar localization of cochlear implant electrodes in adult temporal bones using clinically available computed tomography. Laryngoscope 2010; 120:2277–2283.

Skinner MW, Holden TA, Whiting BR, Voie AH, Brunsden B, Neely JG, et al: In vivo estimates of the position of advanced bionics electrode arrays in the human cochlea. Ann Otol Rhinol Laryngol 2007;116:2–24.

Tan BYB, Gluth MB, Statham EL, Eikelboom RH, Atlas MD: Mobile and landline telephone performance outcomes among telephone-using cochlear implant recipients. Otolaryngol Head Neck Surg 2012;146:283–288.

Telmesani LM, Said NM: Effect of cochlear implant electrode array design on auditory nerve and behavioral response in children. Int J Pediatr Otorhinolaryngol 2015;79:660–665.

Van der Beek FB, Boermans PP, Verbist BM, Briaire JJ, Frijns JHM: Clinical evaluation of the Clarion CII HiFocus 1 with and without positioner. Ear Hear 2005;26:577–592.

Van der Beek FB, Briaire JJ, Van Der Marel KS, Verbist BM, Frijns JHM: Intracochlear position of cochlear implants determined using CT scanning versus fitting levels: higher threshold levels at basal turn. Audiol Neurotol 2016;21:54–67.

Van der Marel KS, Briaire JJ, Wolterbeek R, Snel-Bongers J, Verbist BM, Frijns JHM: Diversity in cochlear morphology and its influence on cochlear implant electrode position. Ear Hear 2014;35:e9–e20.

Venail F, Vieu A, Artieres F, Mondain M, Uziel A: Educational and employment achievements in prelingually deaf children who receive cochlear implants. Arch Otolaryngol Head Neck Surg 2010;136:366–372.

Verbist BM, Skinner MW, Cohen LT, Leake PA, James CJ, Boëx C, et al: Consensus panel on a cochlear coordinate system applicable in histologic, physiologic, and radiologic studies of the human cochlea. Otol Neurotol 2010;31:722–730.

Wanna GB, Noble JH, Carlson ML, Gifford RH, Dietrich MS, Haynes DS, et al: Impact of electrode design and surgical approach on scalar location and cochlear implant outcomes. Laryngoscope 2014;124:S1–S7.

Xu J, Xu SA, Cohen LT, Clark GM: Cochlear view: postoperative radiography for cochlear implantation. Am J Otol 2000;21:49–56.

Yang S, Wang G, Skinner MW, Rubinstein JT, Vannier MW: Localization of cochlear implant electrodes in radiographs. Med Phys 2000;27:775–777.

Zuniga MG, Rivas A, Hedley-Williams A, Gifford RH, Dwyer R, Dawant BM, et al: Tip fold-over in cochlear implantation. Otol Neurotol 2017;38:199–206.